STRUCTURAL SCIENCE
CRYSTAL ENGINEERING
MATERIALS

Volume 76 (2020)

Supporting information for article:

Five concomitant polymorphs of green fluorescent protein chromophore (GFPc) analogue: understanding variations in photoluminescence with π-stacking interactions

Bhupendra P. Mali, Soumya Ranjan Dash, Shrikant B. Nikam, Anisha Puthuvakkal, Kumar Vanka, Kochunnoonny Manoj and Rajesh G. Gonnade

Contents

E-Z Flipping of GFP

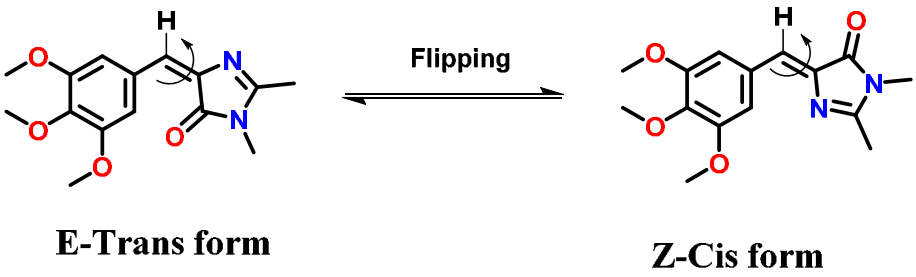

E-Trans form **Z-Cis form**

Figure S1. The schematic representation of E-Z Flipping of GFP chromophore analog.

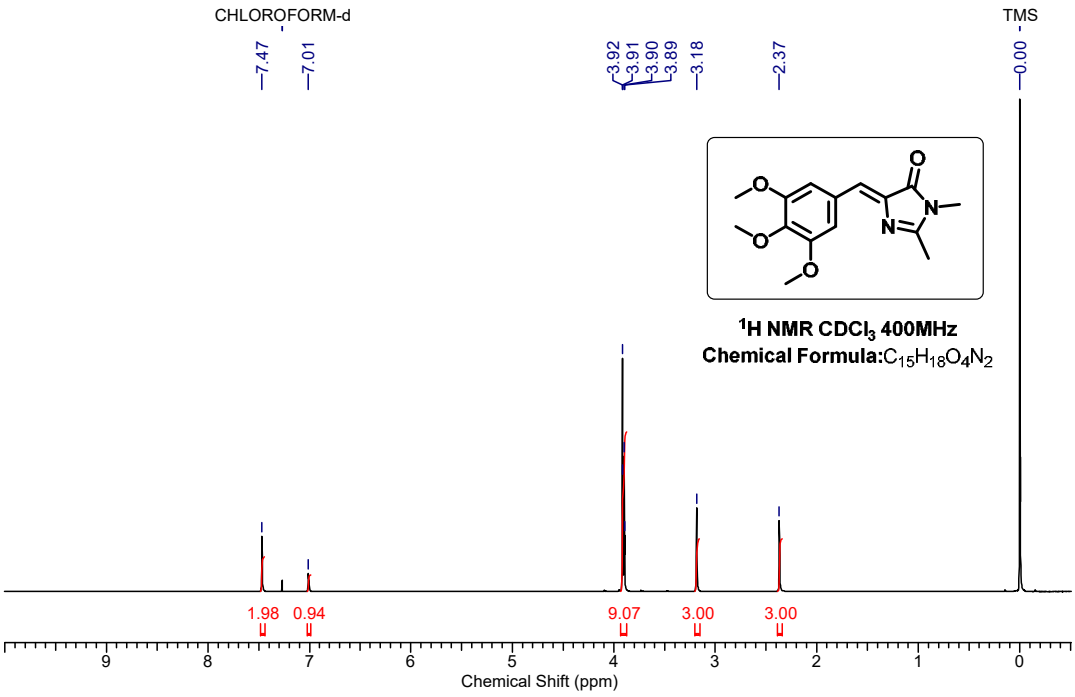

Figure S2. ^{1}H NMR spectrum of **1** in $CDCl_3$.

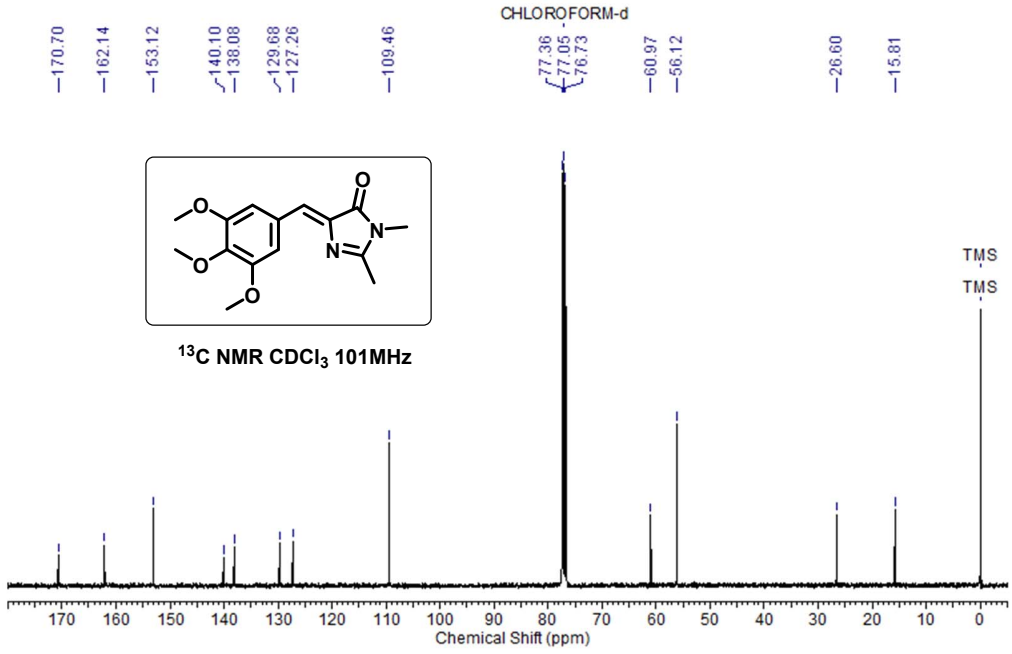

Figure S3. ^{13}C NMR spectrum of **1** in $CDCl_3$.

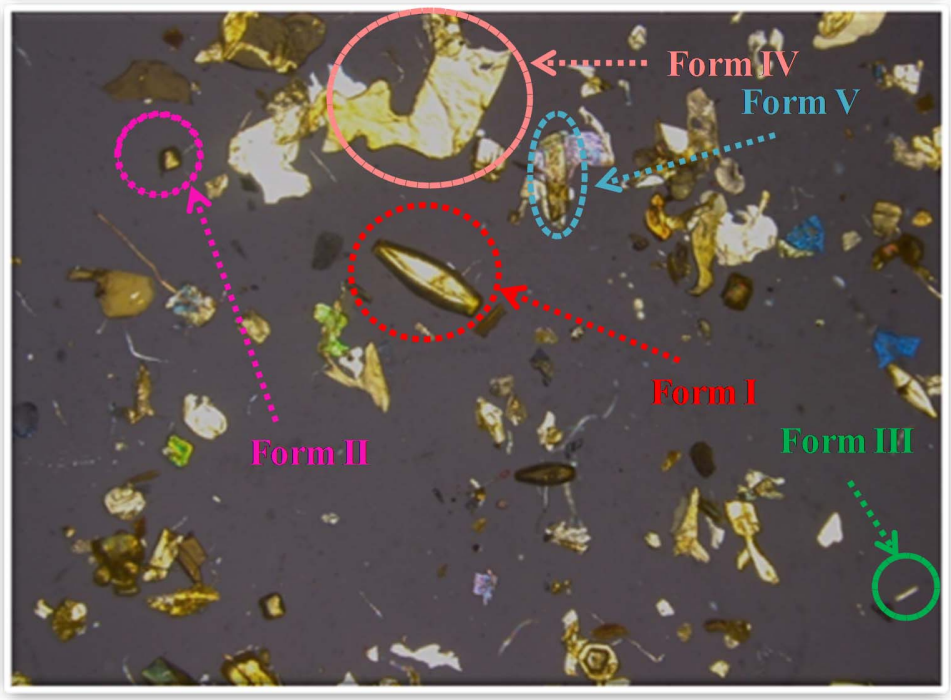

Figure S4. Photomicrographs for concomitant polymorphs of **1**.

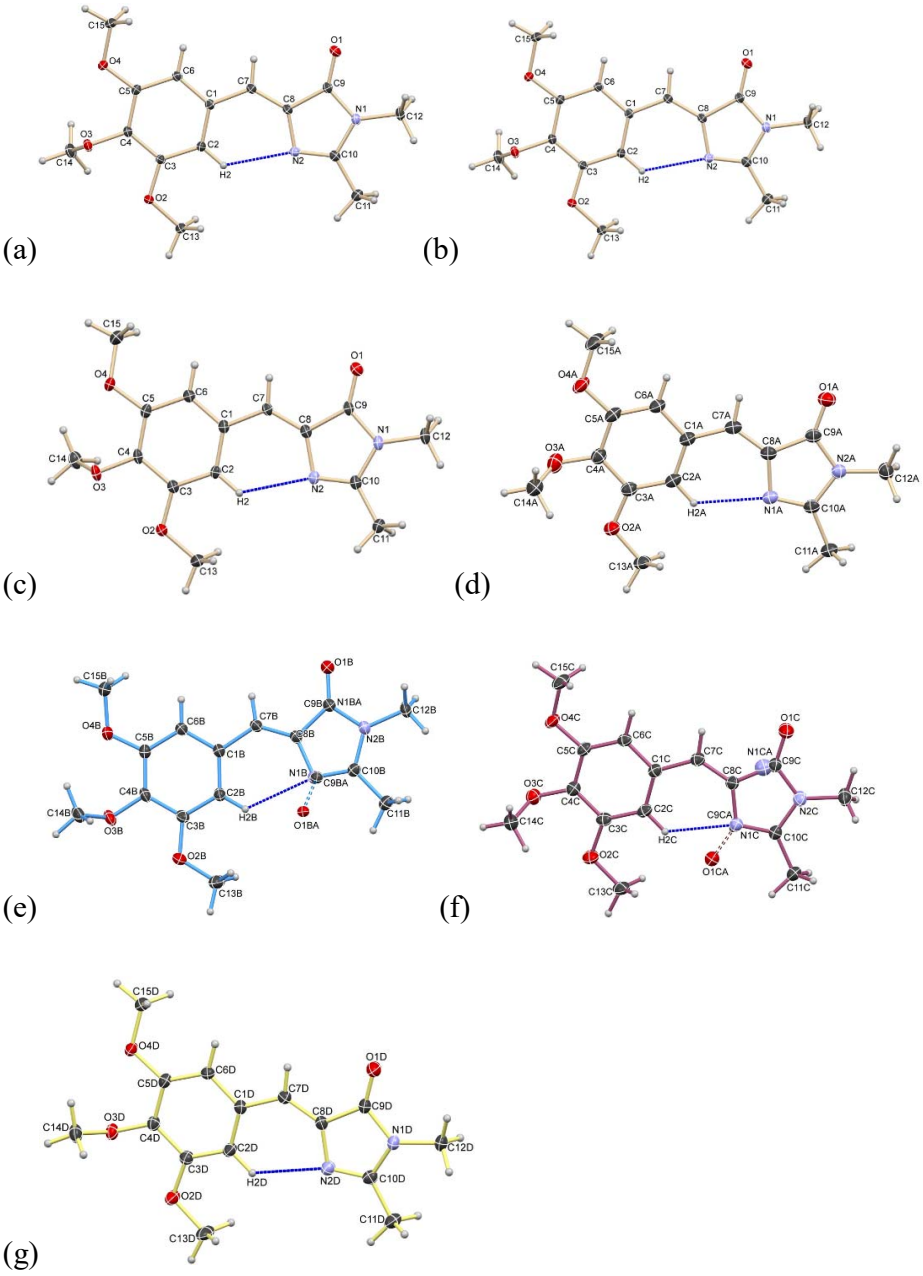

Figure S5. The ORTEP of the molecule of **1** in, (a) Form II, (b) Form III, (c) Form IV and (d), (e), (f), (g) Form V showing the atom-numbering scheme. The thermal ellipsoids are drawn at the 50% probability level, and H atoms are shown as small spheres with arbitrary radii. Molecules labeled with suffix B and C in Form V showed the statistical disorder for the carbonyl group and N atom

of the benzylidene moiety over two positions with approximate occupancies 90% and 10%. The dark blue color dash line indicates the intramolecular C-H···N hydrogen bonding interactions.

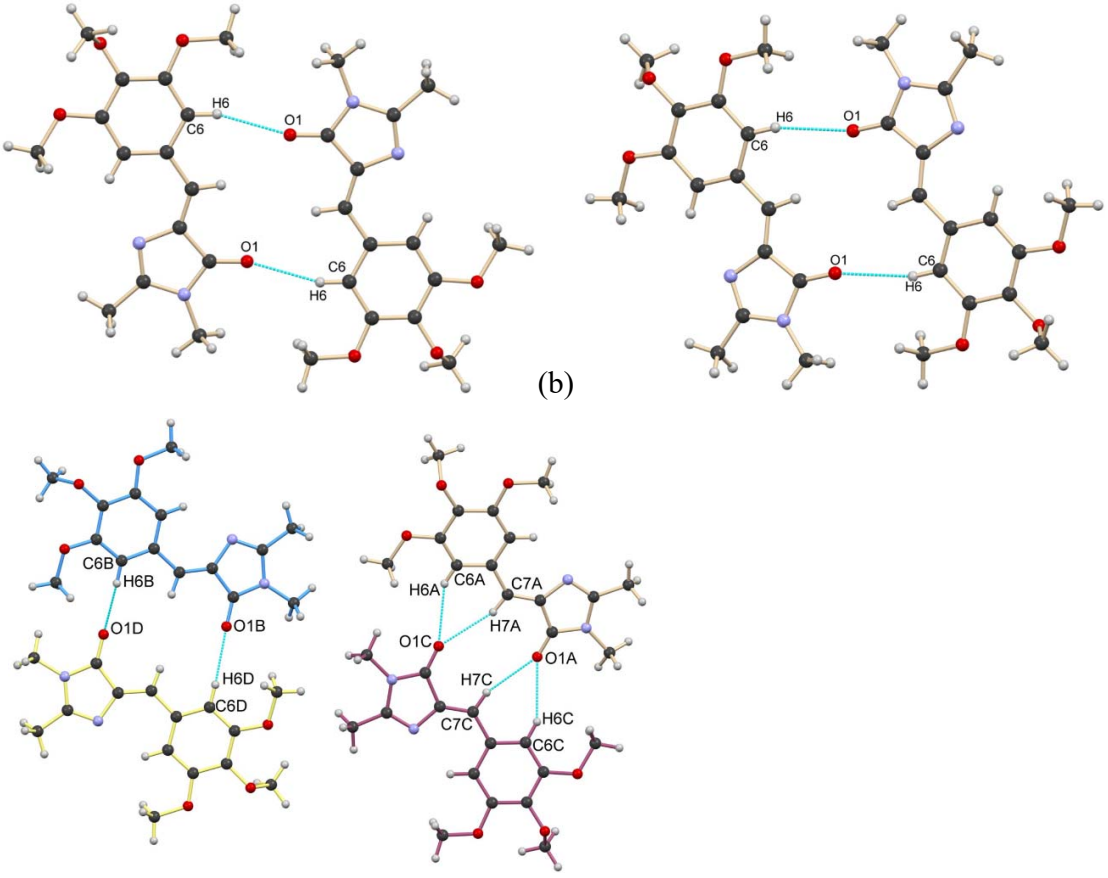

Figure S6. The dimeric association of molecules of 1 using C6-H6···O1 interactions in the polymorphs, (a) Form II, (b) Form III and (c) Form V. In Form V, Molecules B and D and Molecules A and C form the dimeric association.

XPac dissimilarity and isostructurality study between the polymorph

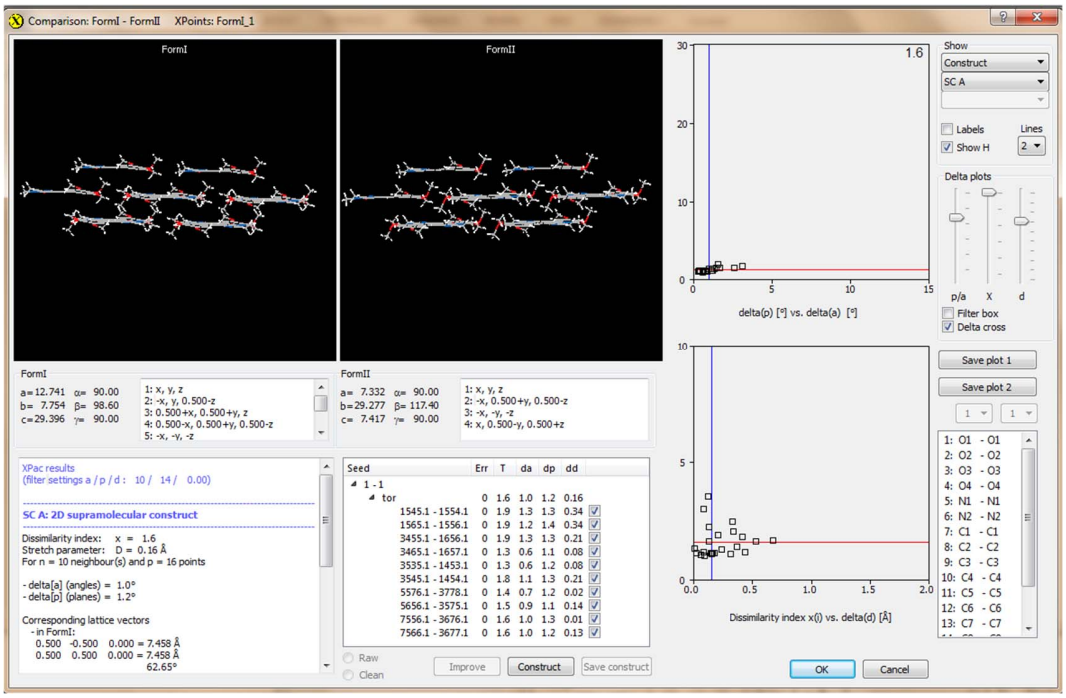

Figure S7. *XPac* calculations for Form I and Form II polymorphs of **1**.

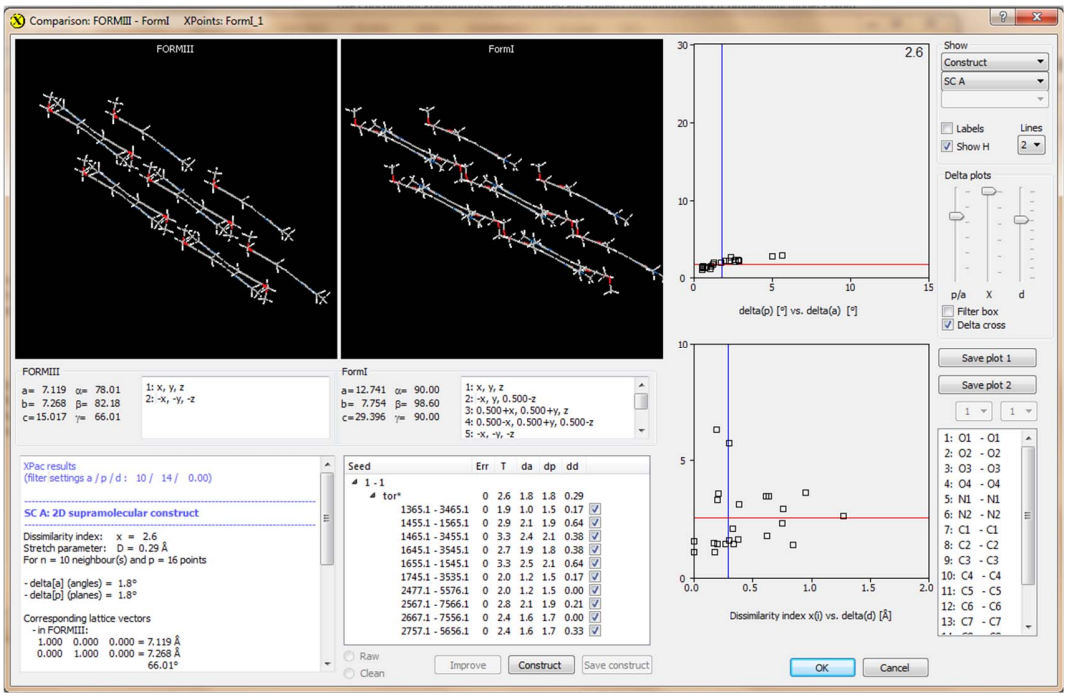

Figure S8. *XPac* calculation Form I and Form III polymorphs of **1**.

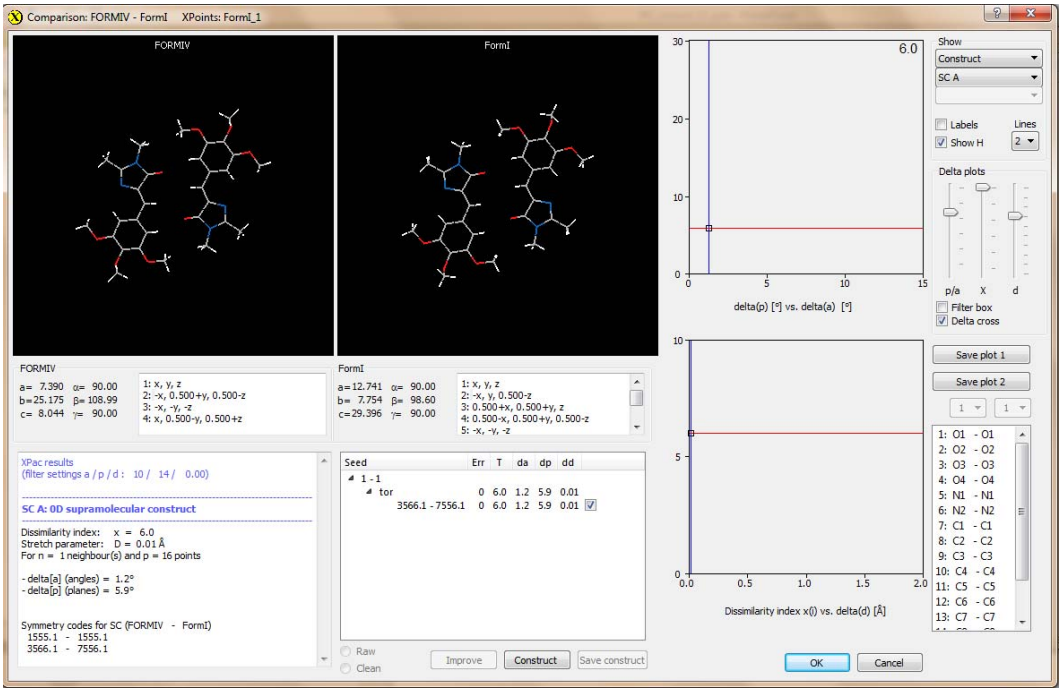

Figure S9. *XPac* calculation for Form I and Form IV polymorphs of **1**.

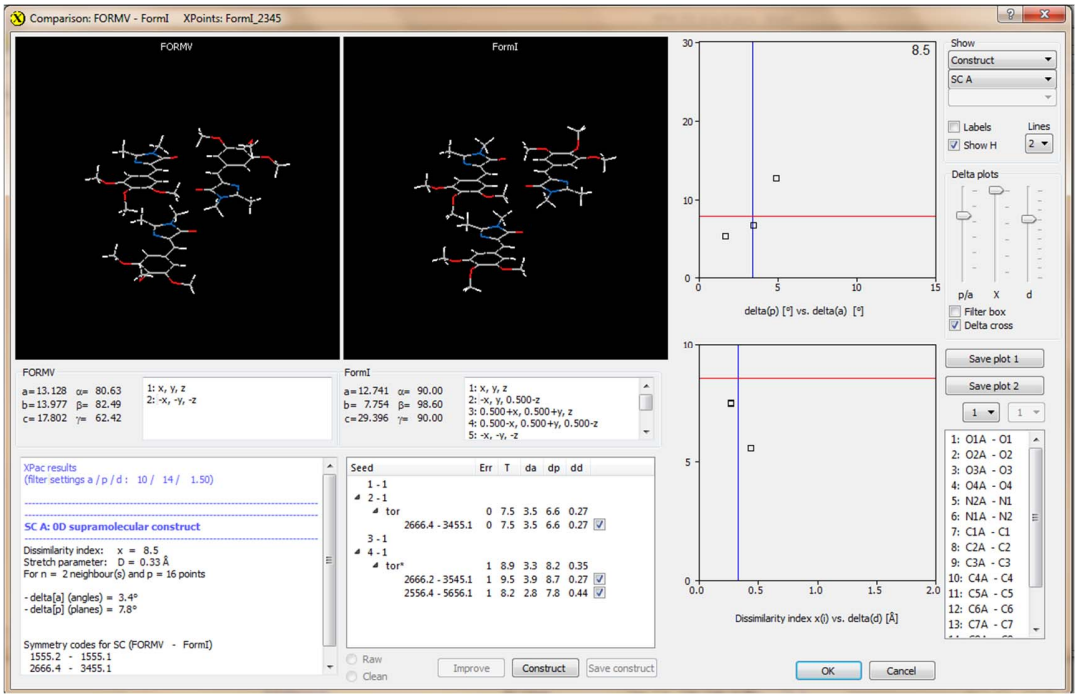

Figure S10. *XPac* calculation for Form I and Form V polymorphs of **1**.

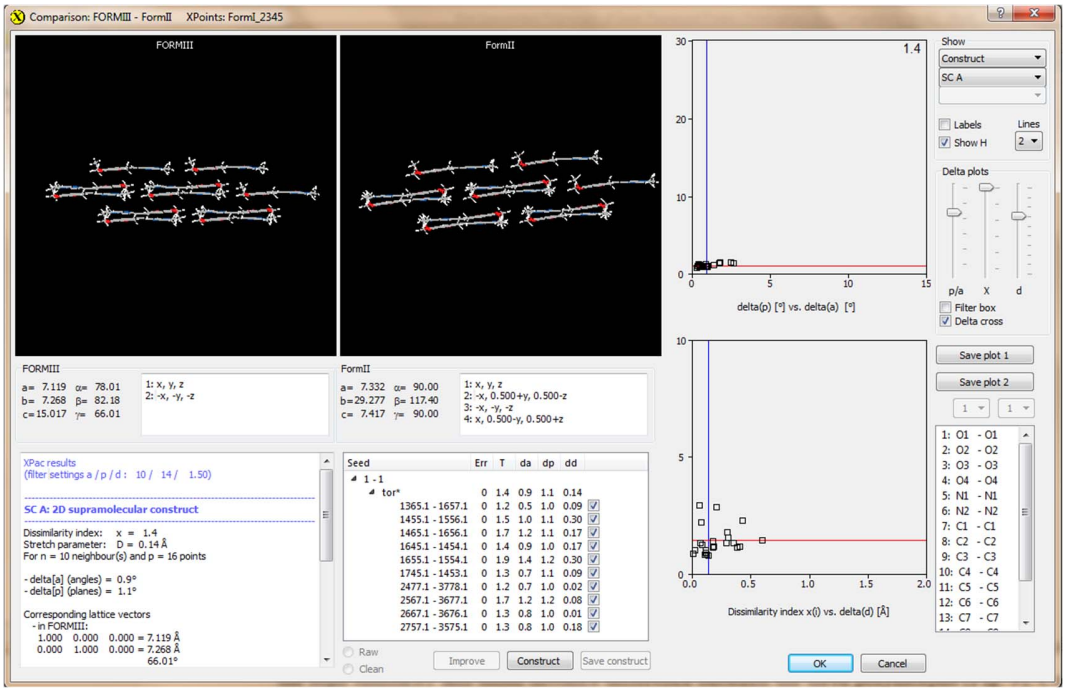

Figure S11. *XPac* calculations for Form II and Form III polymorphs of **1**.

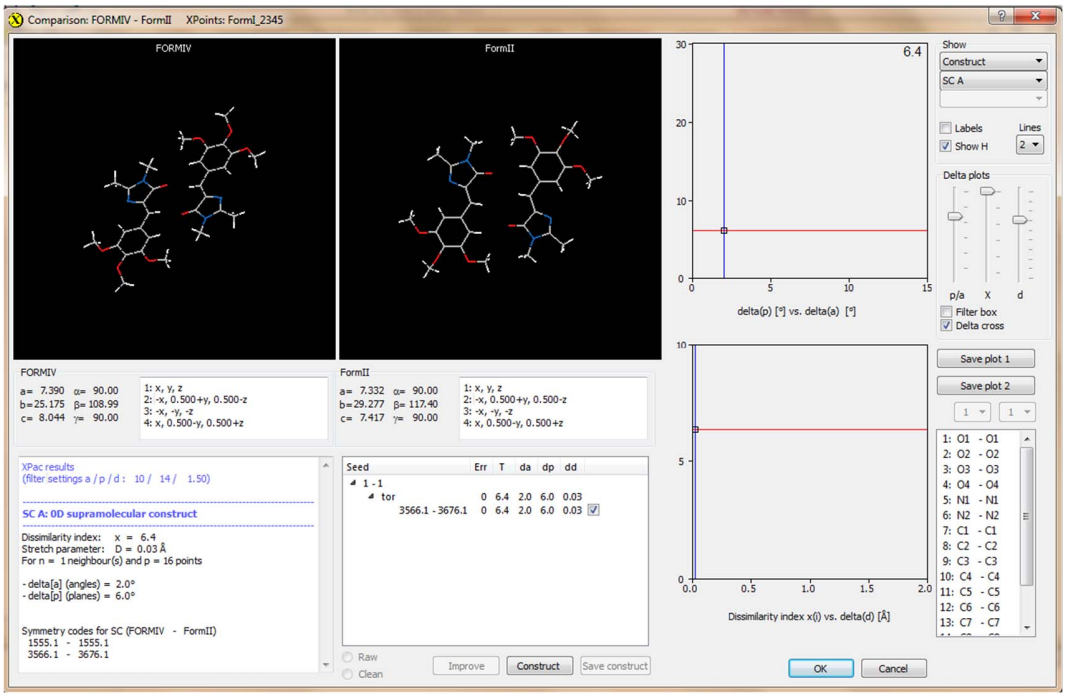

Figure S12. *XPac* calculation for Form II and Form IV polymorphs of **1**.

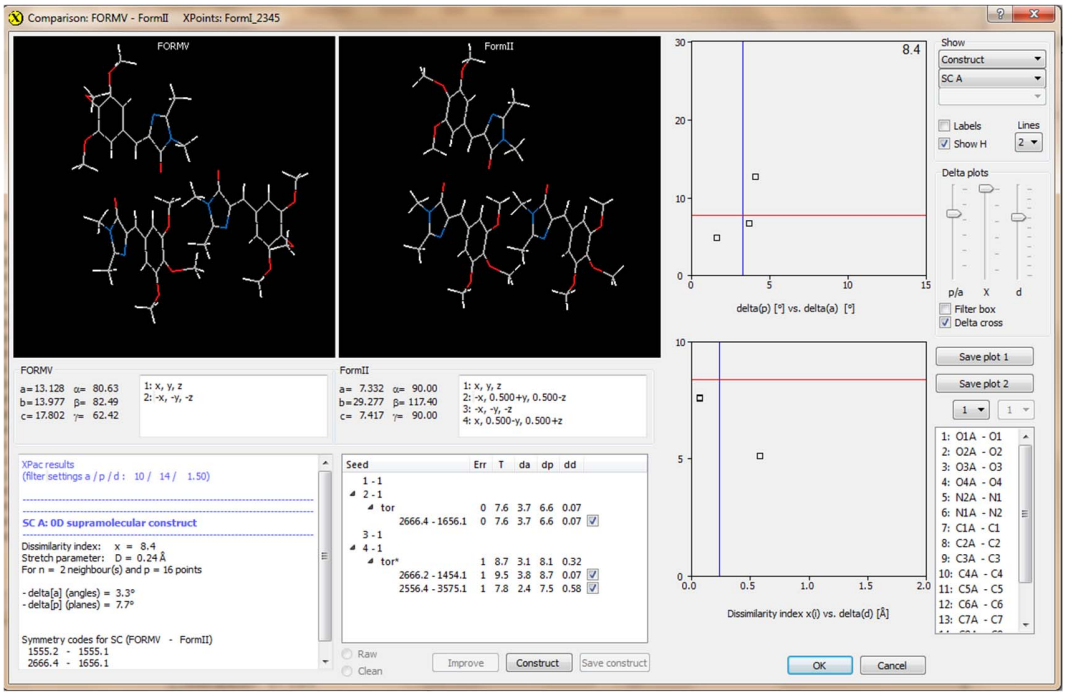

Figure S13. *XPac* calculation for Form II and Form V polymorphs of **1**.

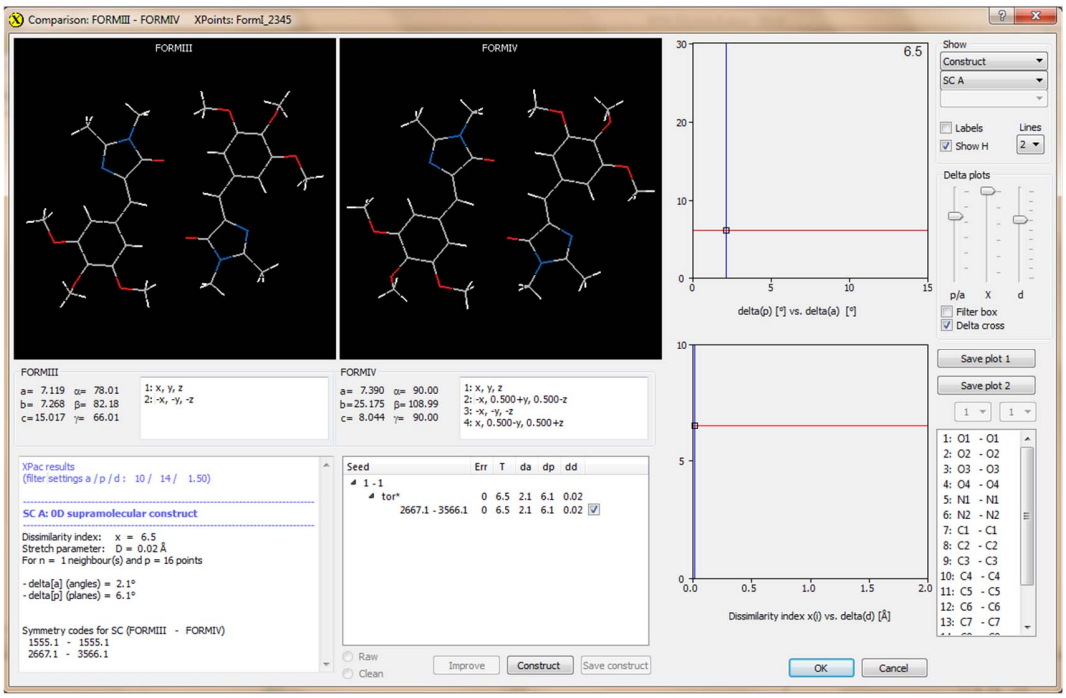

Figure S14. *XPac* calculation for Form III and Form IV polymorphs of **1**.

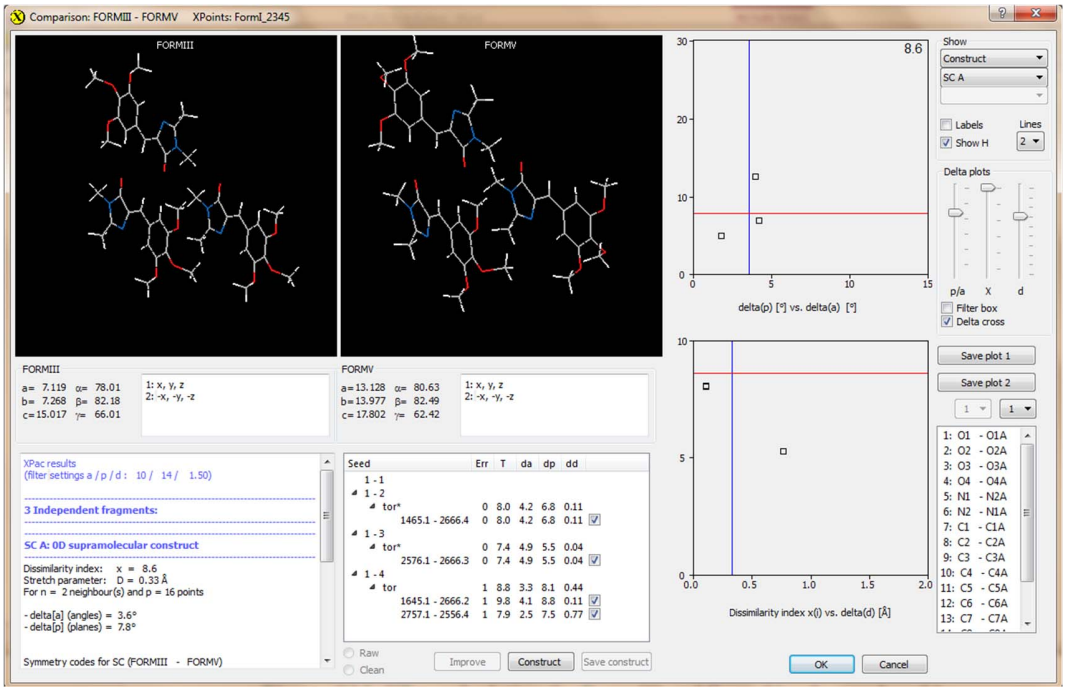

Figure S15. *XPac* calculation for Form III and Form V polymorphs of **1**.

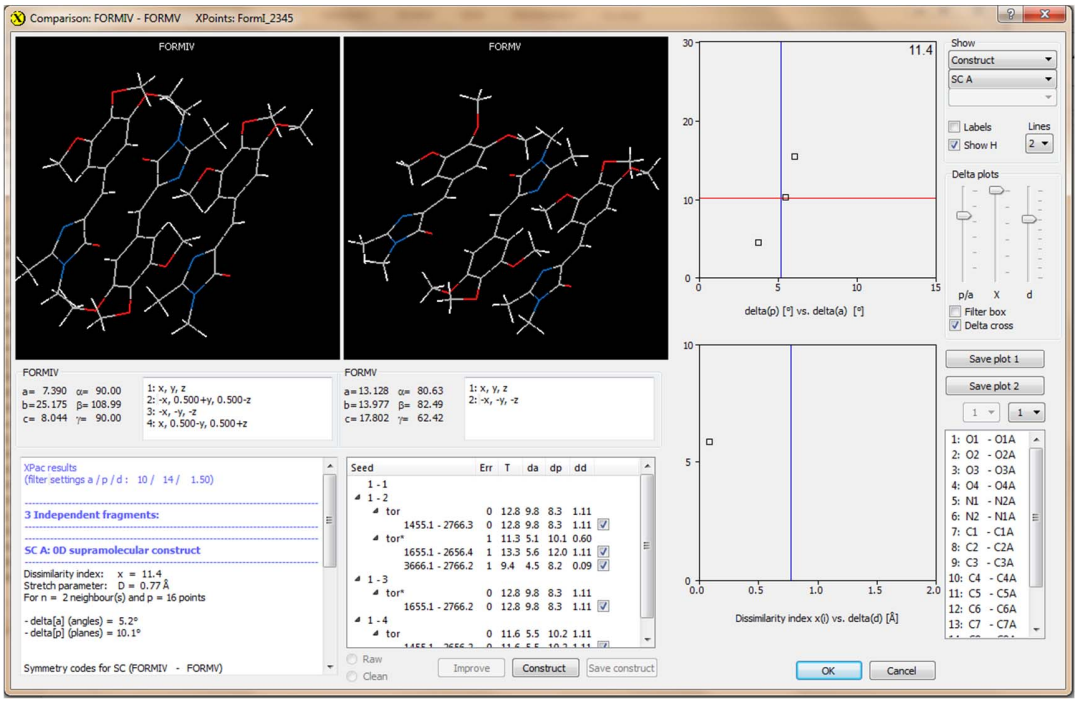

Figure S16. *XPac* calculation for Form IV and Form V polymorphs of **1**.

Hirshfeld Surfaces Analysis

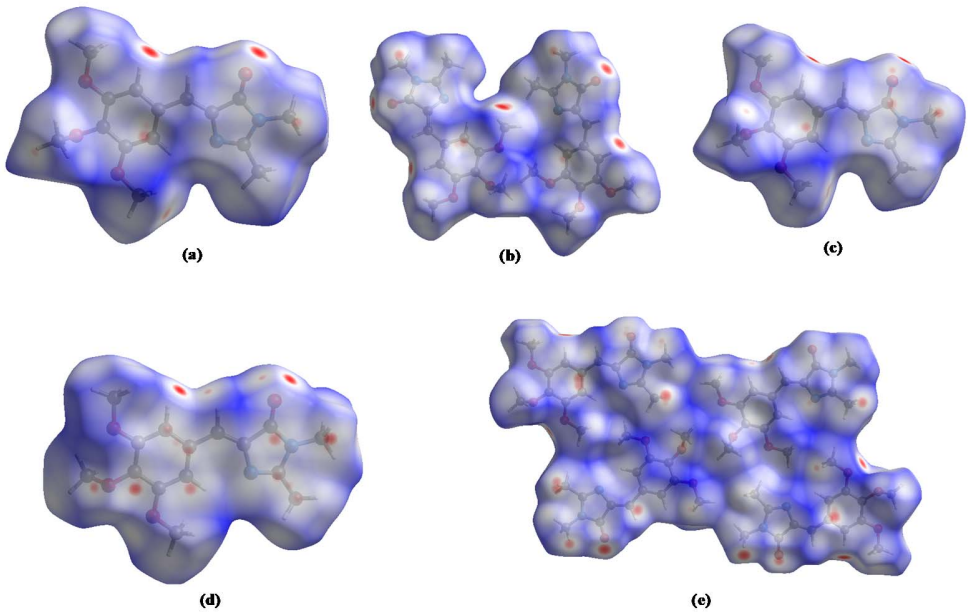

Figure S17. Hirshfeld surfaces plots of all the polymorphs of **1**, (a) Form I, (b) Form I, (e) Form III, (d) Form IV, and (e) Form V.

Hot Stage Microscopy (HSM) Studies

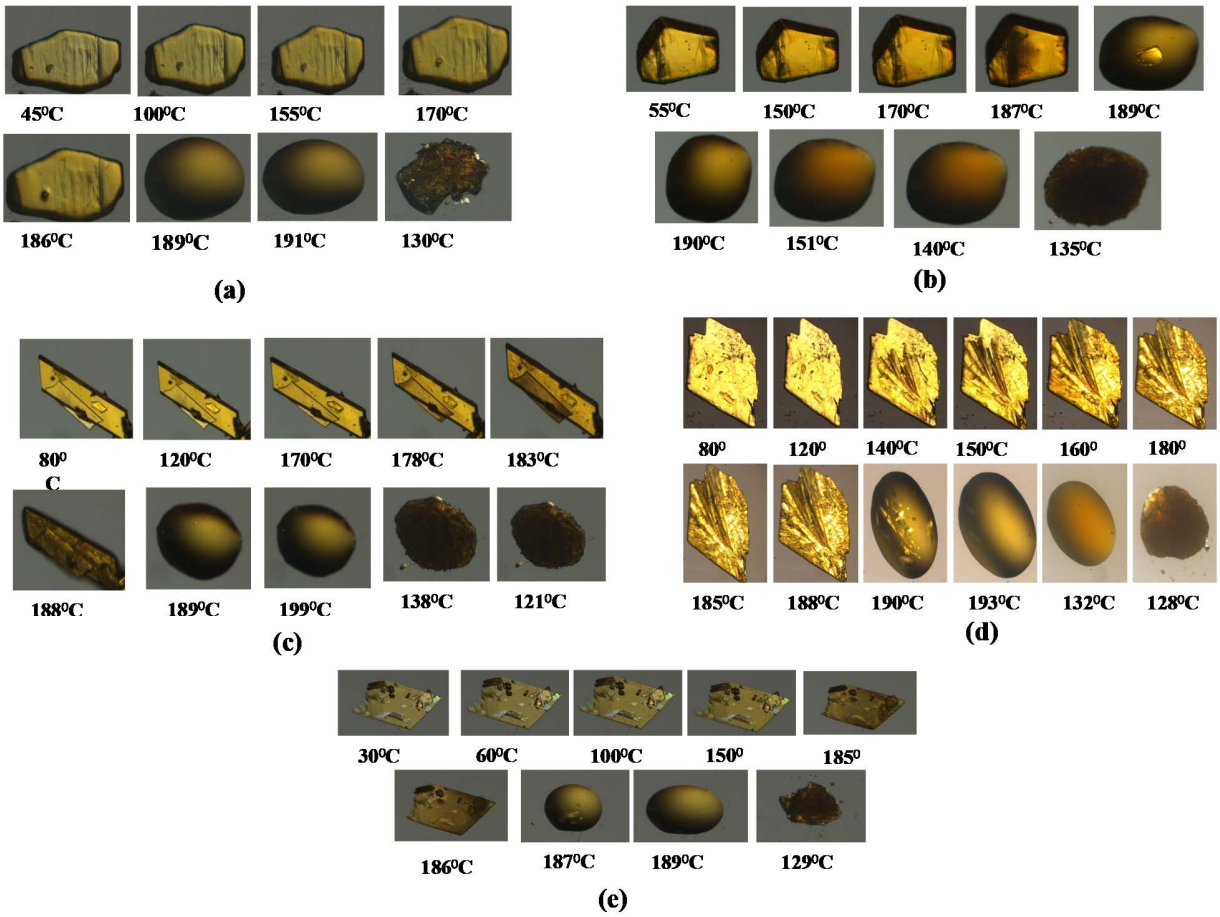

Figure S18. Photomicrographs of the all the polymorphs of 1 captured during hot stage microscopy studies, (a) Form I, (b) Form II, (C) Form III, (d) Form IV, and (e) Form V.

ATR-IR Raman spectroscopy studies

The IR and Raman spectra of solid-state samples, for all polymorphs, are reasonably close. The stretching frequencies observed in IR at 1706(C=O), 2940(C-H) 1400-1600 Aromatic (C=C), 1129 (C-O). Similarly stretching frequencies observed in Raman at 1648(C=O), 1335 (-CH_3), 1164(C-O), 968, 1037 (Aromatic ring) 719-792(C-C).

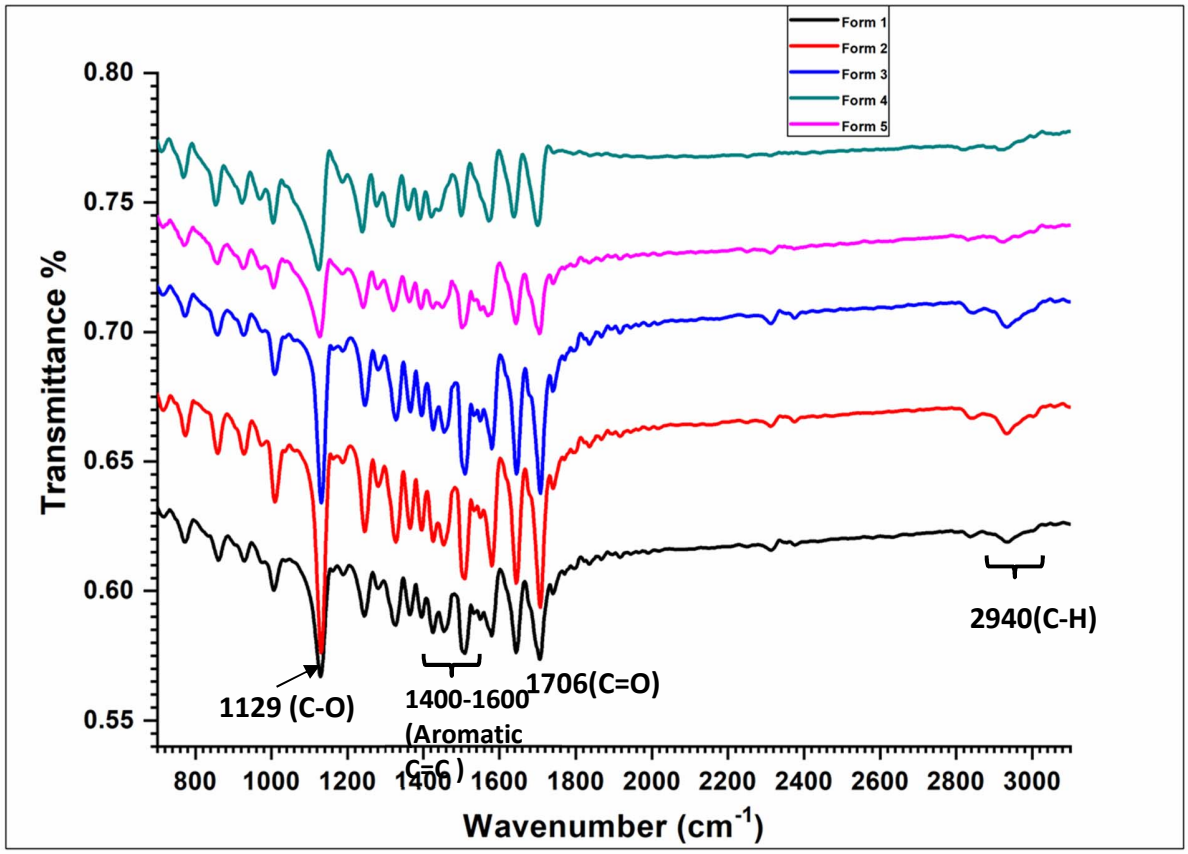

Figure S19. Comparison of IR spectra of all the polymorphs of **1**.

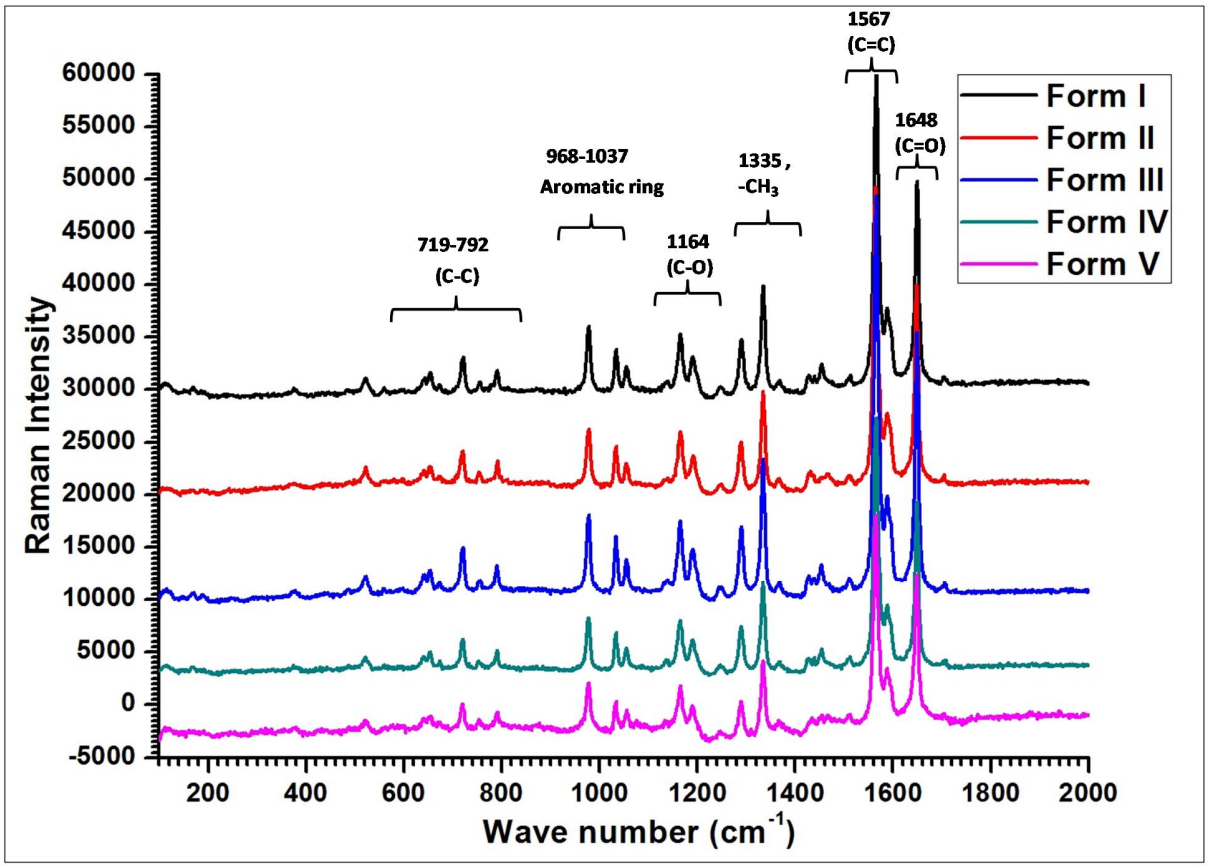

Figure S20. Comparison of Raman spectra of all the polymorphs of **1**.

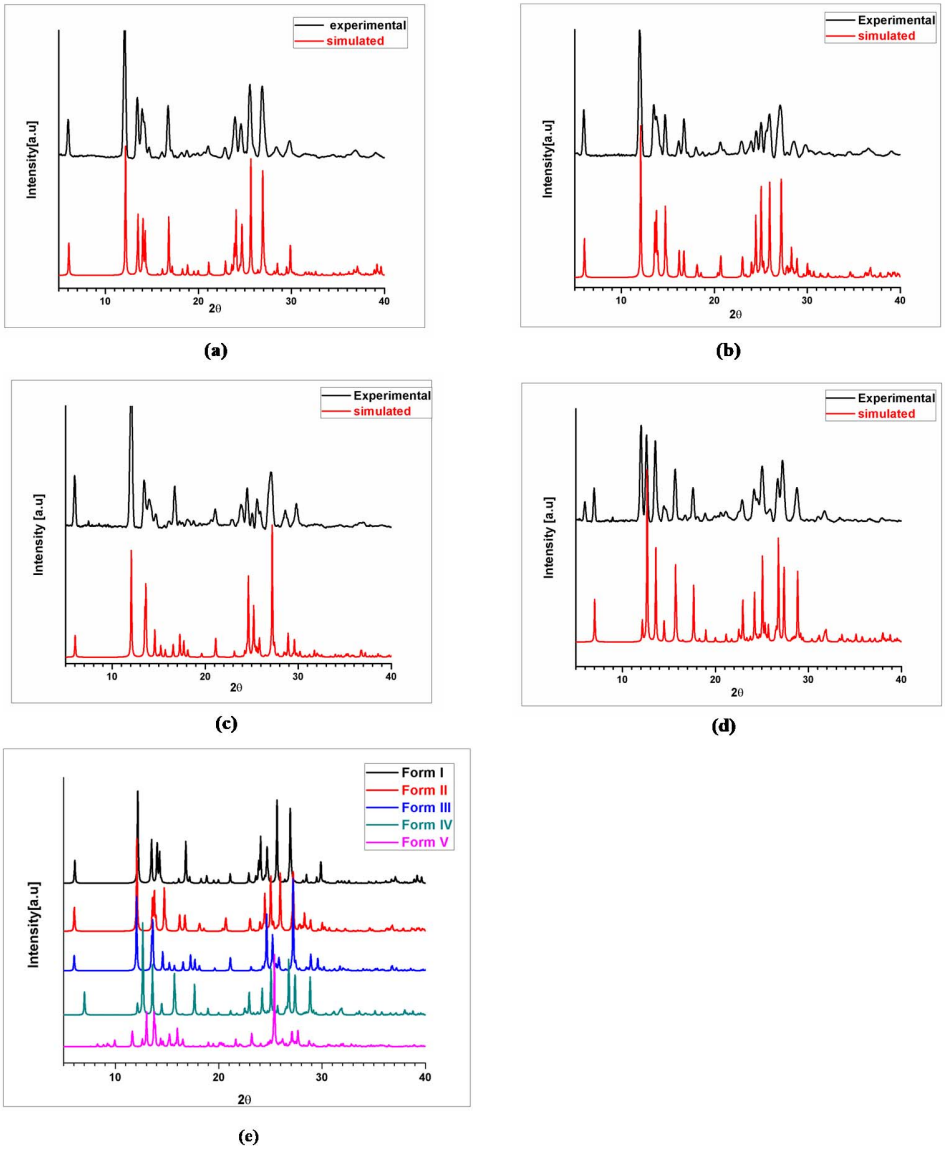

Figure S21. Overlay of experimental (black) and calculated (red) PXRD patterns of all the polymorphs of **1**, (a) Form I (b) Form II, (c) Form III and (d) Form IV and (e) Overlay of the simulated PXRD patterns for all five polymorphs Form I (black), Form II (red), Form III (blue), Form IV (green) and Form V (magenta).

Photophysical study

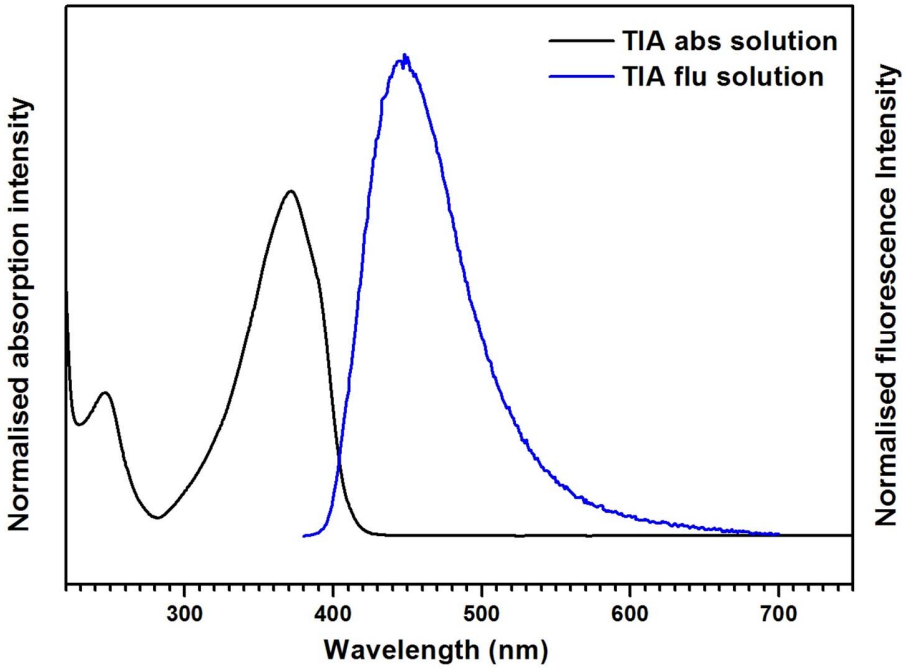

Figure S22. Normalized absorption and fluorescence spectra (excited at 371 nm) in DCM solution.

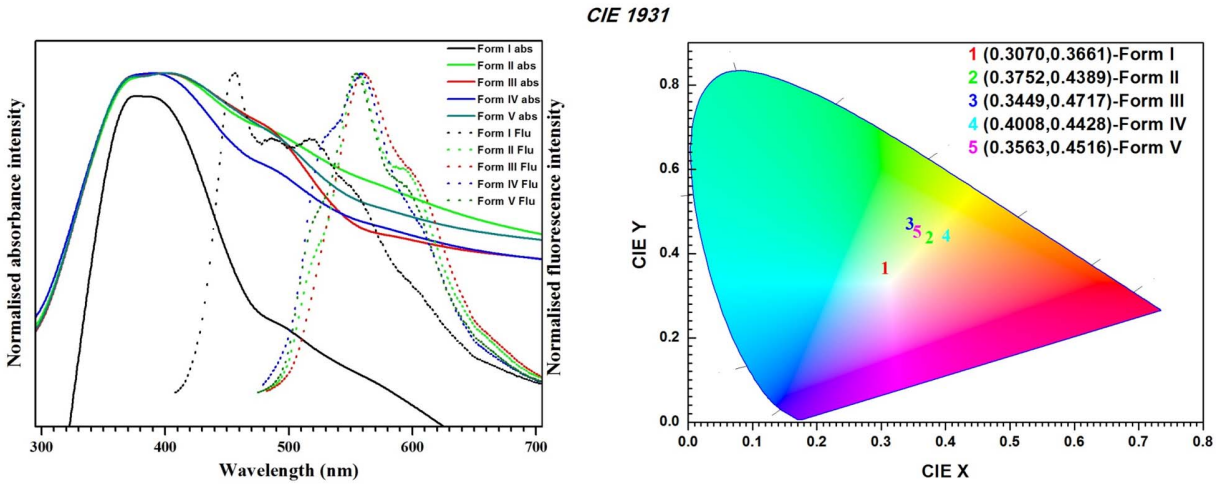

Figure S23. (a) Normalized absorption and fluorescence spectra (excited at 360 nm) and (b) the corresponding coordinates and positions on the CIE chromaticity diagram for all the polymorphs of **1**.

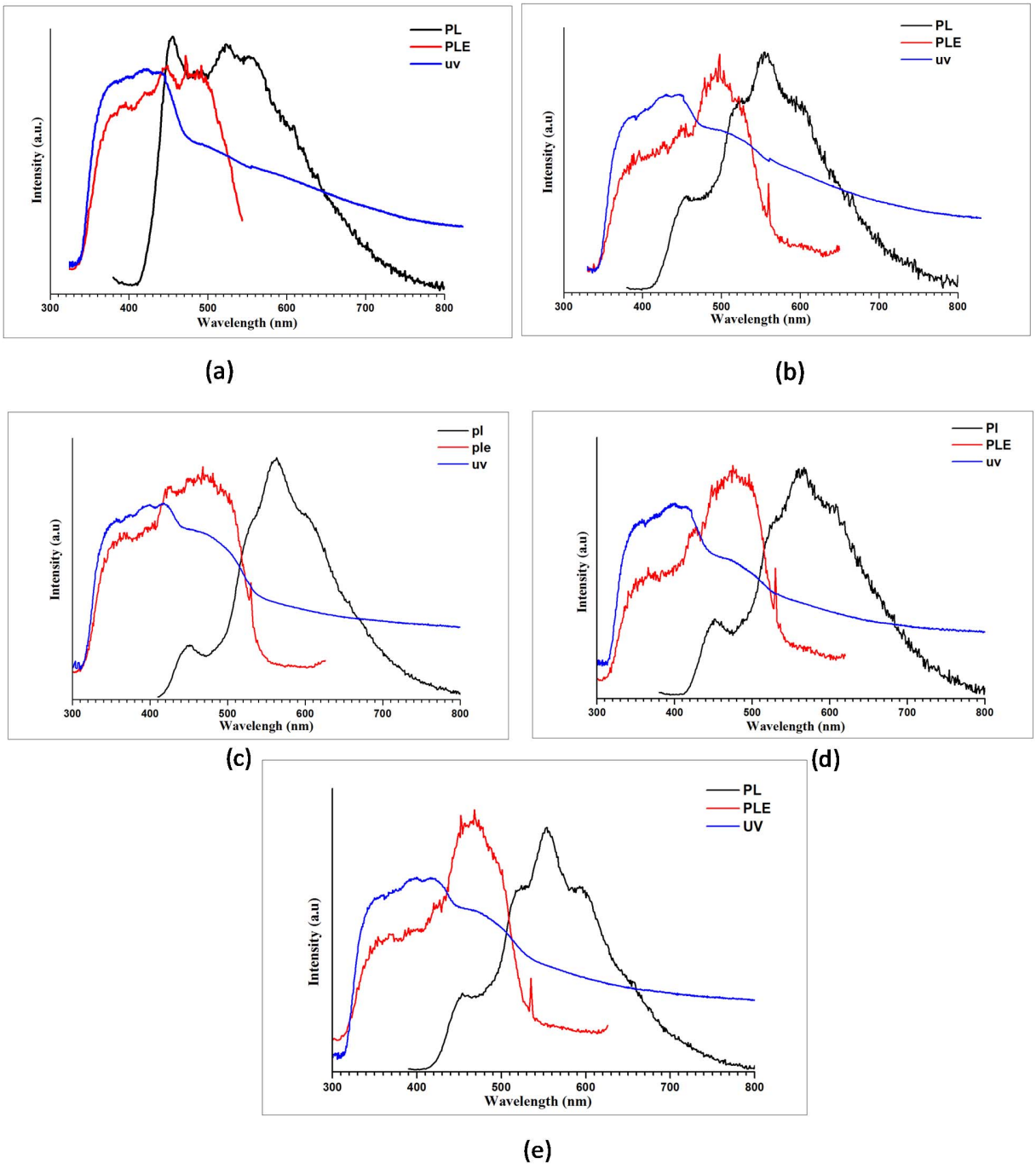

Figure S24. Photoluminescence (at λ=360 nm), photoluminescence excitation (at λ=550 nm) and UV absorption spectra for all the polymorphs of 1, (a) Form I, (b) Form II, (C) Form III, (d) Form IV and (e) Form V.

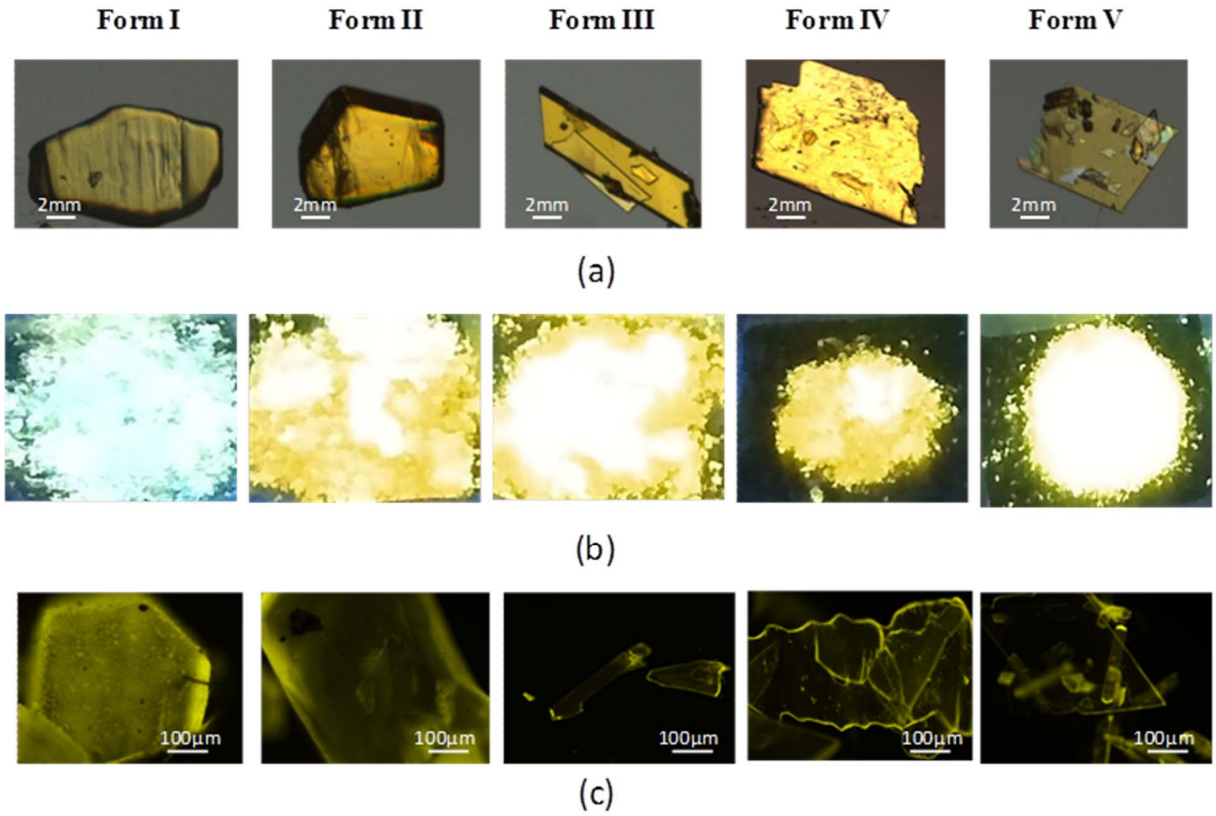

Figure S25. Photomicrograph of all the polymorphs of **1**, Form I to Form V from left to right, (a) optical photomicrographs, (b) photomicrographs under UV light and (c) fluorescence microscope images captured using filters set (20 Rhodamin shift-free Ex BP 546/12, BS FT 560, EM Bp 575-565.) while the yellow color was given using the pseudocolor option.

Time-Resolved PL Decay Studies

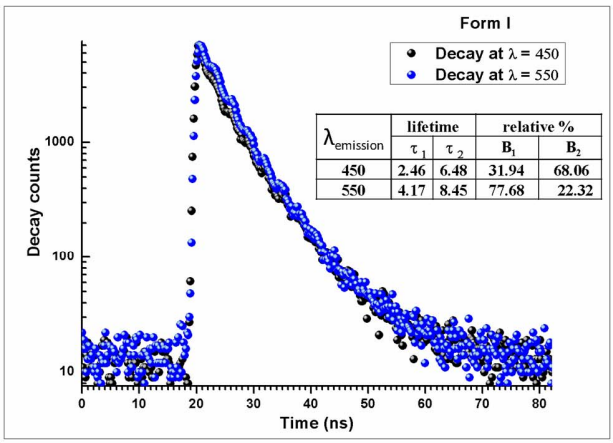

$\lambda_{emission}$	lifetime		relative %	
	τ_1	τ_2	B_1	B_2
450	2.46	6.48	31.94	68.06
550	4.17	8.45	77.68	22.32

(a)

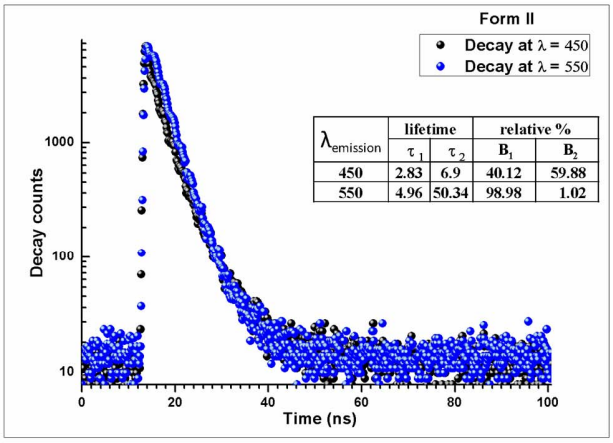

$\lambda_{emission}$	lifetime		relative %	
	τ_1	τ_2	B_1	B_2
450	2.83	6.9	40.12	59.88
550	4.96	50.34	98.98	1.02

(b)

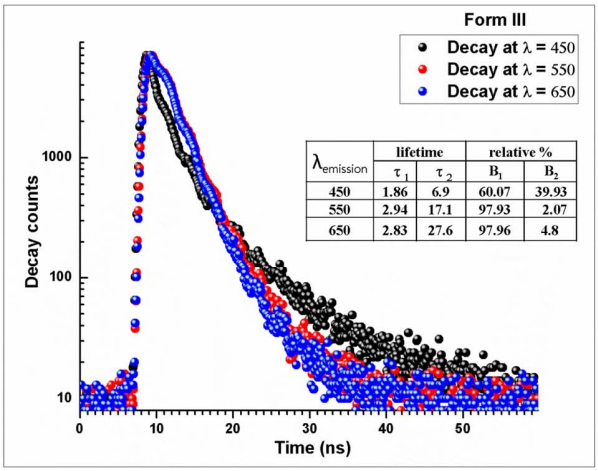

$\lambda_{emission}$	lifetime		relative %	
	τ_1	τ_2	B_1	B_2
450	1.86	6.9	60.07	39.93
550	2.94	17.1	97.93	2.07
650	2.83	27.6	97.96	4.8

(c)

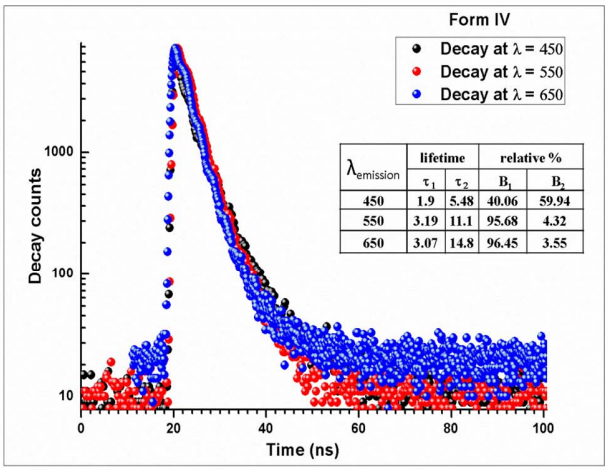

$\lambda_{emission}$	lifetime		relative %	
	τ_1	τ_2	B_1	B_2
450	1.9	5.48	40.06	59.94
550	3.19	11.1	95.68	4.32
650	3.07	14.8	96.45	3.55

(d)

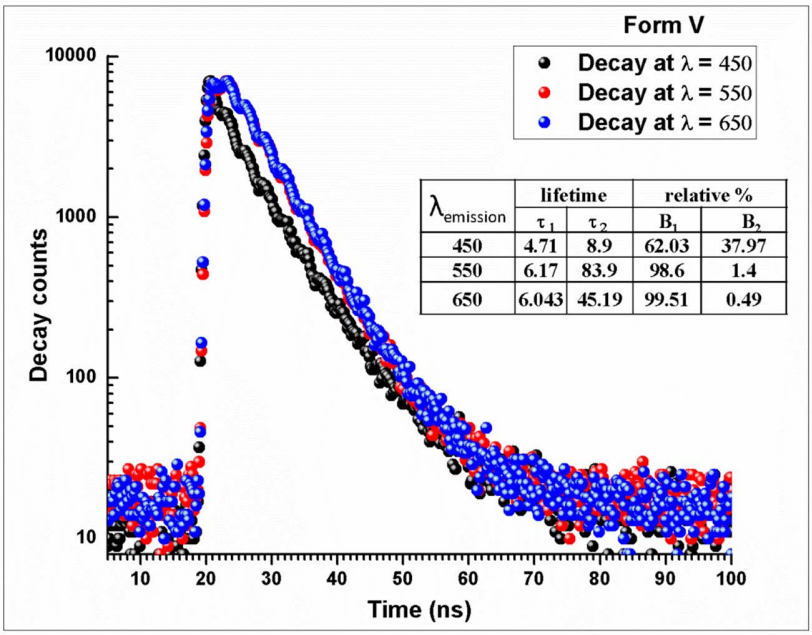

$\lambda_{emission}$	lifetime		relative %	
	τ_1	τ_2	B_1	B_2
450	4.71	8.9	62.03	37.97
550	6.17	83.9	98.6	1.4
650	6.043	45.19	99.51	0.49

(e)

Figure S26. Room temperature time-resolved PL decay curves for all the polymorphs of **1**, (a) Form I, (b) Form II, (C) Form III, (d) Form IV, and (e) Form V.

Calculations of Photophysical Parameters

The photophysical parametres were calculated using following equations:

$\tau_{ave} = a_1 (\tau_1)^2 + a_2 (\tau_2)^2 / a_1 \tau_1 + a_2 \tau_2$
$K_r = \Phi_F / \tau_F$
$K_{nr} = 1/(\tau_F) - K_r$

where,
K_r = Radiative rate constant of fluorescence
K_{nr} = Non-radiative rate constant of fluorescence
Φ_F = Fluorescence quantum yield
τ_F = Fluorescence lifetime

Bandgap calculations:
The bandgap calculation is carried out by the following Davis-Mott relation(tau-plot),

$\alpha h\nu = A (h\nu - Eg)^n$

Where,
A = Energy independent constant
Eg = Optical energy gap
α = Absorption coefficient
n - Denotes the nature of transition

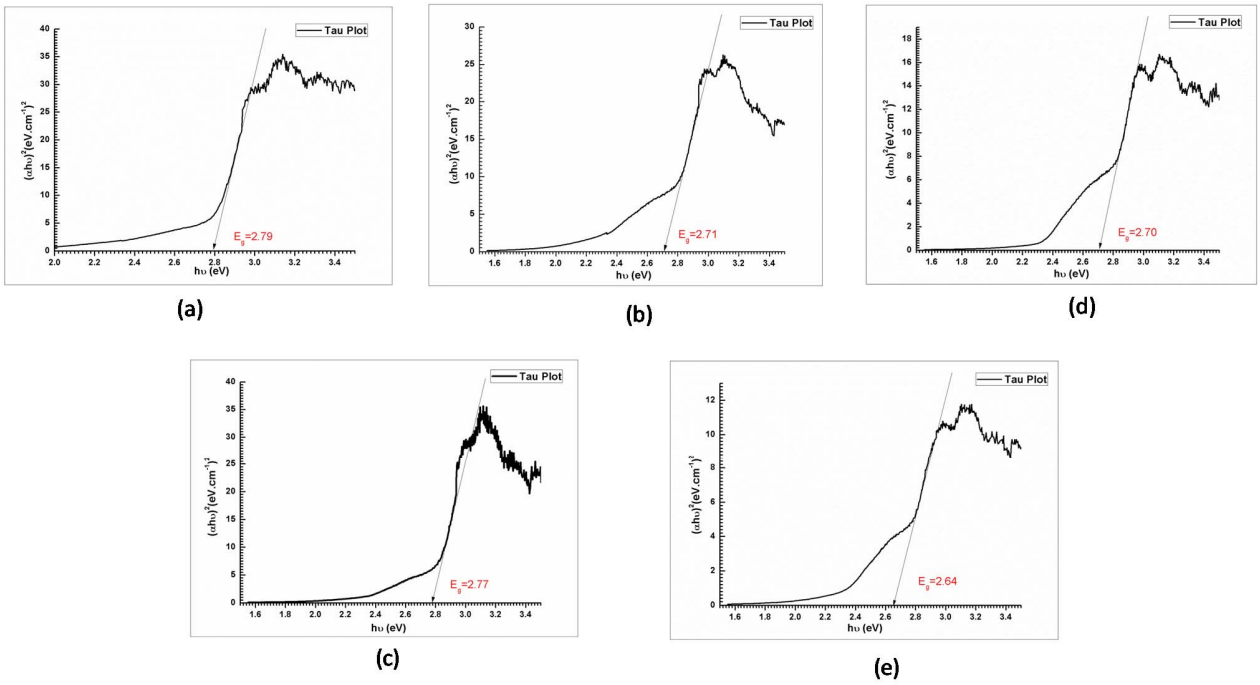

Figure S27. Tauc plot of UV-visible absorption data for the calculation of bandgap energy of all the polymorphs of **1**, (a) Form I, (b) Form II, (C) Form III, (d) Form IV and (e) Form V.

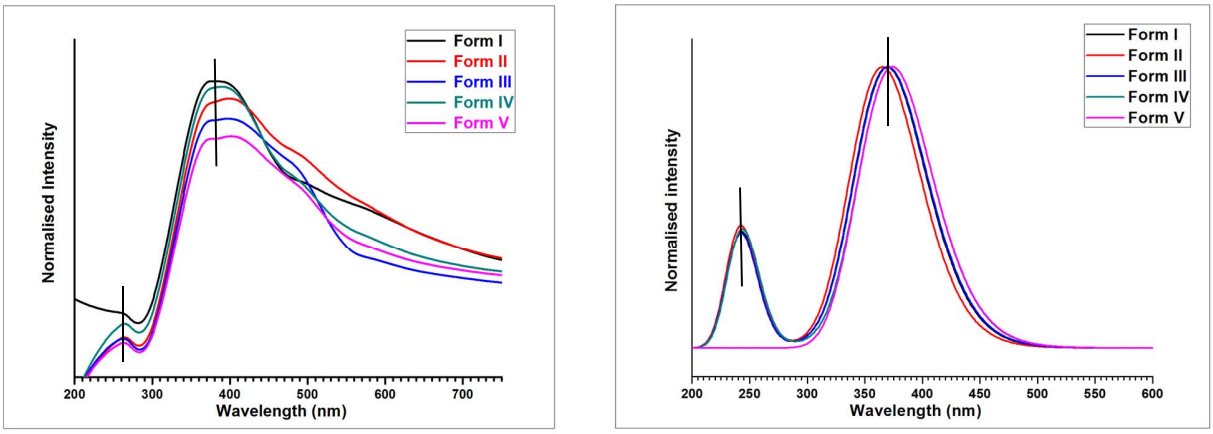

Figure S28. (a) The experimental normalized UV-visible spectra and (b) theoretical normalized UV-visible spectra calculated by TD-DFT for the polymorph of **1**.

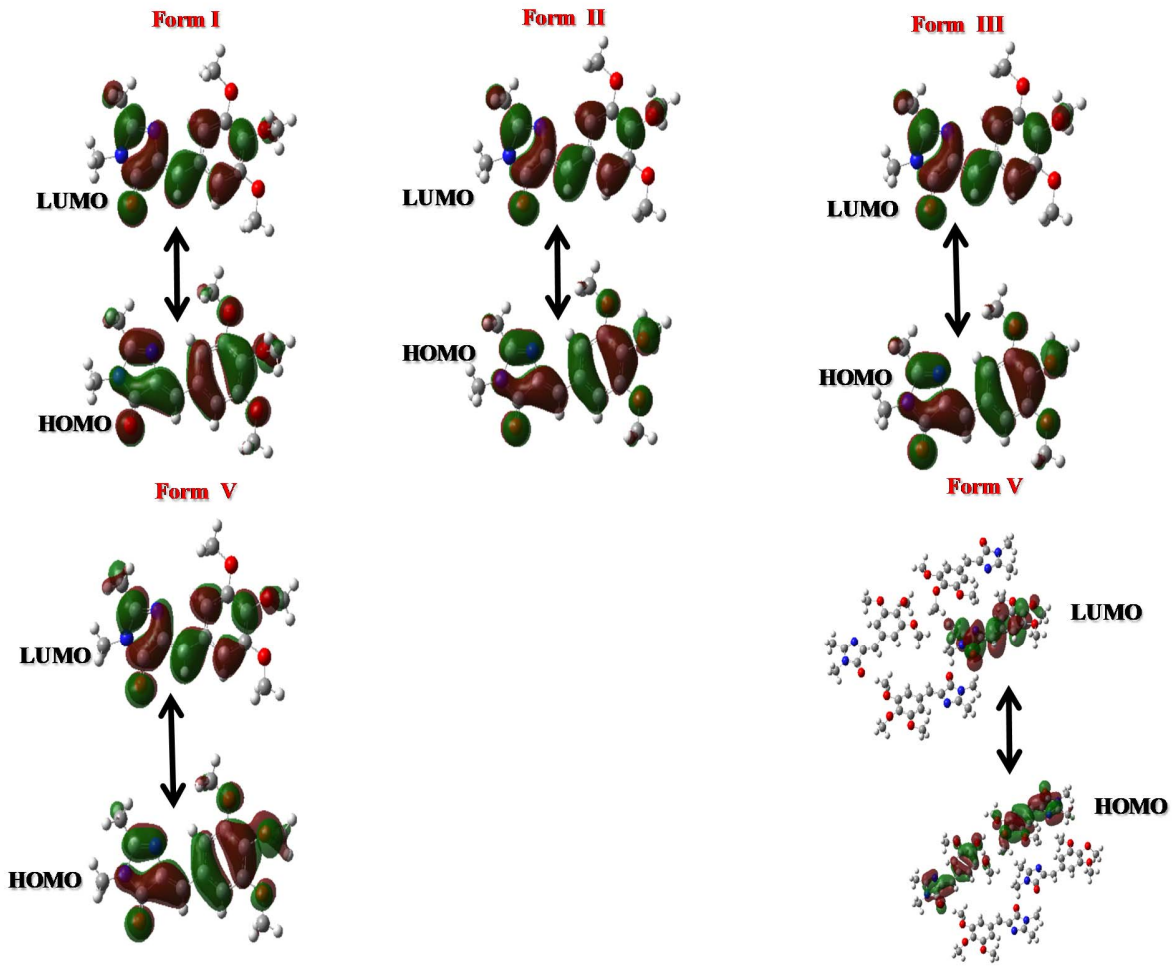

Figure S29. Calculated molecular orbital amplitude plots and energy levels of HOMOs and LUMOs for all the polymorphs of **1** estimated using the Gaussian 09 program with B3LYP/6-311G++(d,p), B97D3/6-311G++(d,p) level of theory and TD-DFT with B3LYP/6-311G++(d,p) level theory.

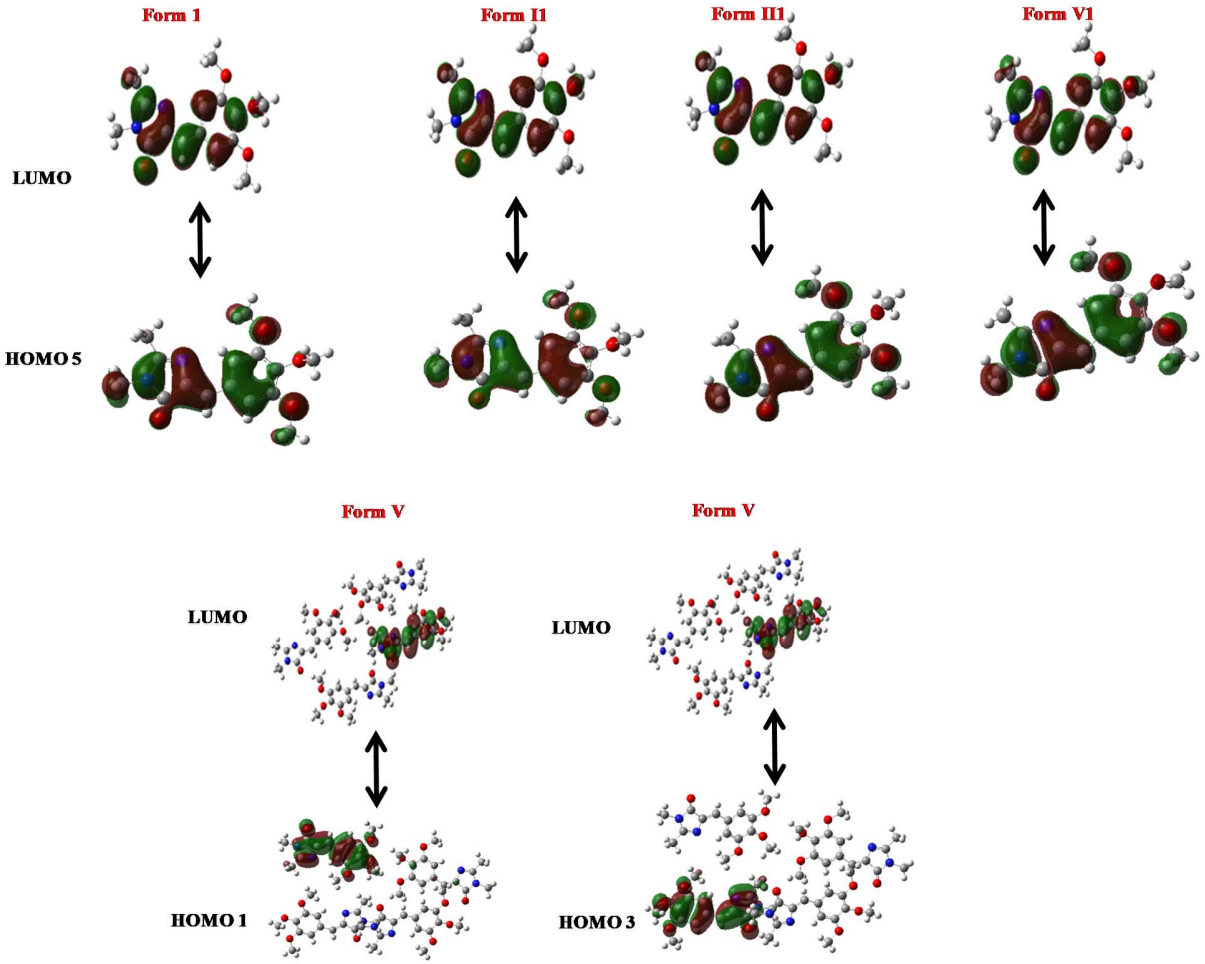

Figure S30. Calculated molecular orbital amplitude plots and energy levels of HOMOs and LUMOs for all the polymorphs of **1** estimated using the Gaussian 09 program TD-DFT with B3LYP/6-311G++(d,p) level theory.

Table S1. Bandgap and transition values for polymorphs of **1**.

Polymorph	Experimental Tau plot (eV/nm)	B3LYP/6-311G++(d,p) (eV/nm)	B97D3/6-311G++(d,p) (eV/nm)	TD-DFT B3LYP/6-311G++(d,p)			
				Transition 1 (eV/nm)	Involved Orbitals	Transition 2 (eV/nm)	Involved Orbitals
Form I	2.79/444.4	3.48/356.3	2.23/555.9	3.34/370.8	HOMO to LUMO	5.06/244.8	HOMO-5 to LUMO
Form II	2.71/457.5	3.53/351.2	2.28/543.8	3.37/368.0	HOMO to LUMO	5.08/243.9	HOMO-5 to LUMO
Form III	2.70/459.20	3.47/357.7	2.22/558.4	3.33/372.8	HOMO to LUMO	5.08/243.9	HOMO-5 to LUMO
Form IV	2.77 /447.6	3.43/360.7	2.19/566.1	3.31/374.4	HOMO to LUMO	5.04/245.9	HOMO-5 to LUMO
Form V	2.64/466.1	3.35/369.2	2.122/584.2	3.05/405.9	HOMO -1 to LUMO	3.33/372.5	HOMO-3 to LUMO